# A Simple Model for Power Consumption in Gassed and Boiling Stirred Vessels

**Alessandro Paglianti, Maria Fujasova, and Giuseppina Montante**
Dept. of Chemical, Mining and Environmental Engineering, University of Bologna, Viale Risorgimento 2, Bologna I-40136, Italy

*DOI 10.1002/aic.11414*
*Published online January 29, 2008 in Wiley InterScience (www.interscience.wiley.com).*

*The aim of this work is to investigate the influence of the main geometrical and hydrodynamic characteristics of gas–liquid stirred tanks on the ventilated cavities forming at the rear of impeller blades and the effect of their size on power consumption. The experimental part of the work was carried in a standard baffled vessel, mechanically stirred with a Rushton turbine. The influence of the sparger diameter on the cavity dimensions and the power consumption was evaluated first, using two different gas spargers. The experimental data confirm that the gas distributor plays an important role on the interactions between the gas–liquid mixture and the impeller. On the modeling side, a simplified correlation to predict the cavity size is developed, that is based on the analogy with the phenomenon of ventilated cavity formation at the rear of vehicles traveling through water. After testing its consistency by adopting available literature data, the correlation is implemented in a mechanistic model for evaluating the power consumption for aerated modern turbines as well as stirred boiling systems, and acceptable predictions are obtained.* © 2008 American Institute of Chemical Engineers *AIChE J,* 54: 646–656, 2008

*Keywords: ventilated cavity, gas–liquid systems, boiling systems, power consumption, mechanistic model, radial impellers*

## Introduction

In the application of stirred vessels to gas–liquid systems, the proper estimation of the hydrodynamics of the two-phase mixture in the turbine region is a critical task. In fact, the formation of ventilated cavities behind the blades strongly influences the apparatus performance, due to their impact on power consumption, gas hold-up distribution, interfacial area, and interphase mass transfer rate.[1–6] So far, several works concerned the study of gas cavity formation mainly in Rushton turbines, while limited information is available on other impeller types.[7,8]

A number of previous works provide recommendations useful for design purposes about the most suitable stirred vessel geometrical configuration for achieving the best results in gas handling capability, power drawn, efficiency in gas dispersion, and mass transfer performances.[9] Also, attention has been devoted to the gas sparger geometry and its position, that were found to affect the aerated stirred tank performances.[8,10,11]

Overall, such guidelines are mainly based on experimental data obtained in vessels of specific impeller type and gas sparger designs, while comprehensive models that describe the effect of geometrical parameters on the stirred vessel hydrodynamic and transport variables are still scarcely available. Besides, computational fluid dynamic (CFD) simulations of gas–liquid stirred tanks could provide detailed information about the fundamental flow characteristics in stirred vessel of any geometrical configuration, at any scale and operating conditions. So far, fair predictions of gas hold-

Correspondence concerning this article should be addressed to A. Paglianti at alessandro.paglianti@mail.ing.unibo.it.

Current address of M. Fujasova: Institute of Chemical Process Fundamentals, Academy of Sciences of the Czech Republic, Rozvojova 2, 165 02 Prague 6 - Suchdol, Czech Republic.

up[12,13] and gas–liquid velocities[14] have been obtained from CFD modeling, while the formation of gas cavity behind the blades cannot yet be simulated properly.[13] Therefore, at present, when the ventilated cavities form at the impeller blades, their effect on the hydrodynamics in the vicinity of the impeller and on other related variables can be taken into account only using experimental data and/or empirical correlations.

As pertains power consumption, its dependency on cavity structure has been widely investigated, while predictive correlations for evaluating the effect of cavity size on power consumption are still lacking. To the best of our knowledge, the only attempt to relate these two quantities was performed by Paglianti et al.,[15] who developed a mechanistic model for power consumption that requires a closure relationship for the evaluation of the cavity size.

Unfortunately, scarce data are available to date on the cavity size, and only few models exist for predicting the cavity behavior.[2,16] Indeed, some indications on cavity modeling can be found in a related topic, namely, the study of vehicles traveling through a liquid (water), as many experimental and theoretical papers have been published in that field.[17–19]

Moreover, the approaches for predicting power consumption in nonboiling gassed systems and in boiling nongassed systems are different, notwithstanding the similarities between the ventilated cavities formed during gas dispersion and those developed in unsparged boiling systems.[20]

In this work, the dimension of the gas cavities has been experimentally evaluated for a vessel of standard geometry stirred with a Rushton turbine and gas spargers of two sizes. Although the selected stirred tank is not the optimal one for practical application, it allows to develop a model that is a useful basis for extension to other impellers. The experimental data have therefore been used to tune a model for predicting the cavity size, that has been adopted as the closing relation for the power consumption correlation proposed by Paglianti et al.[15] The model has also been extended to provide predictions for nonboiling and boiling systems stirred by different radial turbines.

## Experimental

The experiments were conducted in a cylindrical vessel, schematically shown in Figure 1, which was mounted vertically, flat bottomed, and open topped. The vessel, of diameter, $T$, equal to 0.48 m, was fully baffled (baffles width, $B = T/10$) and mechanically stirred with a Rushton turbine. The impeller was set at an off-bottom clearance, $C$, equal to 1/2 of the tank diameter; the impeller to tank diameter ratio was equal to 0.31 ($D = 0.151$ m), that is at the lower end of the usual $D/T$ ratios used in gassed reactors. The vessel was filled with the working liquid up to a height, $H$, equal to $T$. Two different ring gas spargers were used: one smaller (SS) and the other larger (LS) than the impeller; therefore, in the former case the gas was sparged directly beneath the impeller while, in the latter case, it was well outside the radius of the impeller swept volume. Each sparger consists of a tube bended in the form of a ring. The SS sparger had a diameter equal to $D_s = 0.09$ m ($D_s = 0.60D$) and its clearance with respect to the vessel bottom was equal to 85 mm ($C_s = 0.18T$); it was provided with 36 holes of 2 mm in diameter,

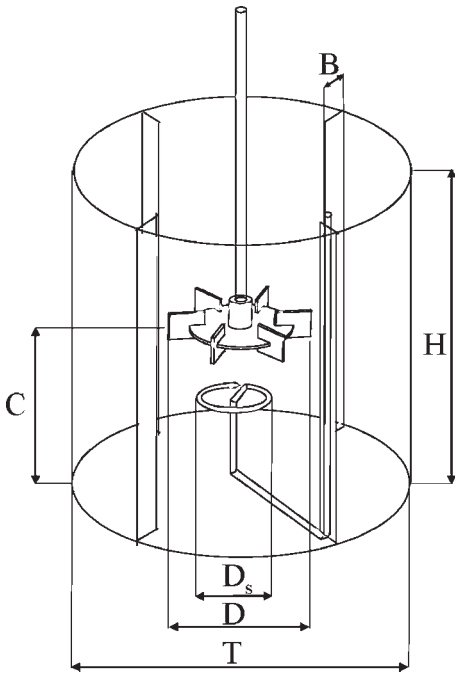


**Figure 1. Geometrical configuration of the stirred vessel.**

equally spaced along the tube upper periphery. The LS had a diameter equal to $D_s = 0.365$ m ($D_s = 2.40D$), a vessel bottom clearance of 45 mm ($C_s = 0.09T$), and 38 holes of 2 mm in diameter on the tube upper periphery.

Though this configuration is not the optimal one and its practical use is nowadays losing importance, this investigated geometry was selected as a reference case for the model development, due to deep knowledge of its hydrodynamics gained in previous works.

The experiments were started by filling the vessel up to the height $H$ with the working liquid, that, in all cases, was de-ionized water at room temperature (coalescent system), and starting the agitation at the selected impeller rotational speed, $N$. Afterward, the gas phase was fed to the stirred tank; the gas flow rate was measured using a HI-TEC mass flow meter. The gas flow rate, $Q_g$, was varied from 1.4 to $14 \times 10^{-4}$ m$^3$/s, which is equivalent to a gas flow number, $Fl_g$, variation from 0.01 to 0.09. $Fl_g$ is defined as the ratio between $Q_g$ and ND.[3] The upper limit of gas flow rate was due to the necessity to obtain clear images for the measurement of the cavity dimensions. As a result, the experiments were performed in fully turbulent conditions ($Re$ equal to about $10^5$) and in the loading regime, covering both the vortex/clinging and the "3-3" cavity structures.

Since the base of the vessel was flat and made of transparent plastic, pictures of the ventilated cavities formed at the rear of the blades could be easily taken without any optical distortion. The pictures were collected with a single frame digital camera. For the cavity size estimation, the analysis of each picture was performed by counting the number of pixels covered by the cavity. The analysis was repeated at least on six pictures for each experimental condition, and a mean value of the measured cavity size was obtained. The mean

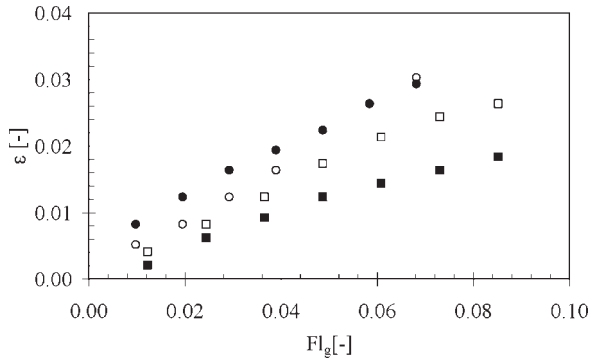


**Figure 2. Effect of the sparger size on the mean void fraction.**

■, SS N = 240 rpm; □, LS N = 240 rpm; ●, SS N = 300 rpm; ○, LS N = 300 rpm.

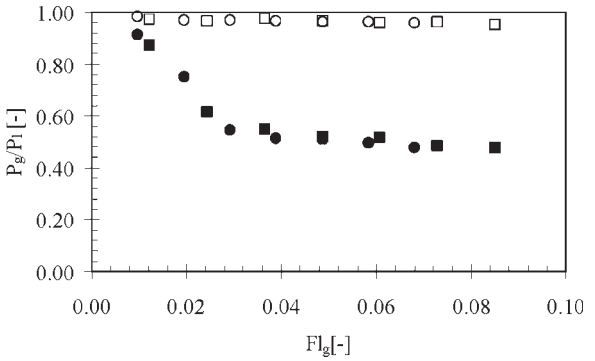


**Figure 3. Effect of the sparger size on the power ratio, $P_g/P_l$.**

■, SS N = 240 rpm; □, LS N = 240 rpm; ●, SS N = 300 rpm; ○, LS N = 300 rpm.

square error in cavity size measurements was equal to about 20% for the SS and to 11% for the LS.

Gassed ($P_g$) and ungassed ($P_l$) power consumption measurements were also performed. The power drawn by the impeller was evaluated by measuring the restraining torque necessary to prevent the motor from rotating with respect to the stationary vessel. The motor was suspended from its top and aligned by means of radial bearings. All the measurements were corrected for no-load friction, which was in fact extremely low.

Finally, mean gas hold-up data were also collected by measuring the liquid level height with and without aeration.

## Results

The experimental data shown in Figure 2 clearly indicate that, with both the LS and the SS spargers and at two different impeller rotational speeds, the mean void fraction varies from almost zero, at the lowest gas flow number, up to 0.03, which corresponds to a quite small mixture density variation (i.e., from 1000 down to 997 kg/m$^3$). Therefore, the performance of the two spargers in terms of overall gas hold-up does not differ significantly. These results confirm that the gas bubbles are approximately the same in number and size at the exit of each gas sparger (the hole diameter is equal to 2 mm in both cases) and presumably they experience the same coalescence phenomena (a coalescent liquid was used). Mass transfer parameters have not been measured in this work, while specific information on the effect of sparger size and position on the volumetric mass transfer coefficient of radial and axial impellers has been recently presented by Sardeing et al.[9] As far as the effect of void fraction is concerned, mass transfer reduction is to be expected when using the LS, as already found in previous investigations.[8] On the other hand, large ring spargers permit to achieve higher specific power input with radial Rushton turbines, thus producing higher turbulent energy dissipation levels, which could enhance mass transfer coefficients. The result of these competing effects depends on the specific operating conditions.[9]

In all the experiments without aeration, power consumption measurements led to a power number value equal to 5.0, steady in the fully turbulent region, as expected. In Figure 3 the effect of the sparger size on the power ratio, $P_g/P_l$, as a function of the gas flow number, $Fl_g$, is shown. As can be observed, for the SS sparger the relative power significantly decreases when increasing $Fl_g$, while the fall of the relative power is considerably less marked for the LS. These results are in agreement with previous data.[3,6,21–23] Since power consumption is controlled by the cavity form,[6] the large difference between the power ratio curves obtained with the two spargers could be considered as an indirect indication of the different size of the cavities formed at the rear of the impeller blades. The gas flow-rate entering the impeller directly from the sparger is much larger with the SS than with the LS and the different gas flow-rate discharged by the turbine probably induces cavities of different size.

The pictures collected from the cavity size measurements show that when the LS is used, the cavities are very small as compared with those formed using the SS at the same gas flow number and with the same impeller blade size. These observations confirm that the quantitative estimation of the cavity size is a fundamental prerequisite for the prediction of power consumption in aerated stirred tanks. The experimental area (bottom view) of a single cavity as a function of the gas flow number is shown in Figure 4. As can be observed, at equal operating conditions, the cavity area obtained with the LS is significantly smaller than that of the cavities formed when the SS was used. In particular, the cavity area varies from 1.5 to 5 cm$^2$ for the LS, while it is equal to 5 and

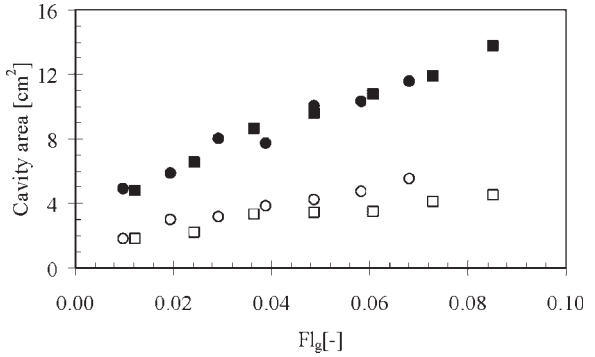


**Figure 4. Experimental cavity area at different gas flow number.**

Symbols as in Figure 2 and 3.

12 $cm^2$ for the SS for the lowest and highest of the investigated gas flow numbers. Overall, the data collected in this work allow to confirm the well known dependency of the overall gas hold-up and power consumption on the phenomenon of cavity formation at the rear of the impeller blades in aerated systems. The main objective of the experiments was to provide a quantitative basis for the development and the validation of the model presented in the following sections.

### *The model for the cavity size estimation*

The ventilated gas cavities can be analyzed using an approach similar to that already developed for the description of the ventilated cavities formed at the rear of vehicles traveling in water,[17–19] as the two phenomena are characterized by strong physical analogies. In addition, artificial ventilation around a body is often adopted for creating and studying the cavitation, due to the dynamic similarities of cavity–liquid interface and of the flow around the cavity.[24] For the same reasons, the theoretical results obtained for cavitating flows can be extended to the description of various ventilated devices.[25]

First of all, a simple criterion for establishing the cavity presence at the rear of an impeller blade has to be identified. In the present work, the results obtained by Brenner[26] will be adopted, who analyzed the point at which the cavity detaches an immerged body, which corresponds to the point at which cavity formation starts, and suggested that gas cavity takes place on body surfaces that are convex viewed from the liquid. This observation precludes the presence of a detachment point, and consequently the presence of the cavity, on concave surfaces. This theoretical result agrees with experimental observations on Scaba SRGT[27] and Chemineer BT-6 impellers.[28] For flat blades, the cavity formation phenomenon is well known,[29] and the detachment point for the large cavities coincides with the blade tip.

In the following, a simple model for predicting large cavity size behind a flat or a convex blade is presented.

Among the operational parameters influencing the ventilated flow problems, the gas flow rate, the free stream pressure, $p_\infty$, and the undisturbed free stream velocity, $U_\infty$, are the most important. The last two parameters can be related through the cavitation (or ventilation) number, $\sigma$, that is defined as:

$$\sigma = \frac{p_\infty - p_c}{\frac{1}{2}\rho_l U_\infty^2} \tag{1}$$

where $p_c$ is the cavity pressure and $\rho_l$ is the liquid density. The cavitation number, that can be obtained from the Navier–Stokes equations by dimensional analysis, describes the ratio of pressure forces and inertial forces. The cavity formation is characterized by a small value of $\sigma$, which in the case of the so-called natural supercavitation is achieved adopting high free stream velocities, while in ventilated conditions it is due to the increase of the cavity pressure.

For the case of stirred vessels, $U_\infty$ can be considered as coincident with the impeller tip velocity, $V_{tip}$, that is known, while the free stream and the cavity pressure are local variables dependent on the particular hydrodynamic and turbulent conditions around the impeller blades. Therefore, the evaluation of $\sigma$ is not straightforward.

If the cavitation number is known, the cavity length can be computed through the well-known results of Garabedian,[17] who faced the study of the cavity flow on the basis of the mathematical solution of a free-boundary variation problem and obtained the shape of the free surface between liquid and gas as a part of the solution. For cavitation numbers lower than 1, the following asymptotic relationship was theoretically derived:

$$\frac{L}{d} = \frac{1}{\sigma}\sqrt{C_D \ln\frac{1}{\sigma}} \tag{2}$$

where $L$ is the cavity length, $d$ is the cavitator characteristic length, and $C_D$ is its drag coefficient. For very low values of $\sigma$, the square root term on the right hand side of Eq. 2 is constant, therefore, it can be simplified as[18]:

$$\sigma = C_1 \frac{d}{L} \tag{3}$$

To identify a further link among the parameters that affect cavity formation, the cavitation number can be related to the gas flow rate leaving the cavity, by introducing the definition of gas entrainment coefficient:

$$\overline{Q} = \frac{\dot{V}}{U_\infty d^2 C_{D0}} \tag{4}$$

where $\dot{V}$ is the volumetric gas flow rate leaving the cavity and $C_{D0}$ is the drag coefficient at zero cavitation number. The entrainment coefficient can be calculated from the cavitation number by the following correlation[18]:

$$\overline{Q} = C_2 \frac{(1+\sigma)}{\sigma}\sqrt{\frac{1}{\sigma}\ln\frac{1}{\sigma}} \tag{5}$$

where $C_2$ is a constant depending on the hydrodynamic regime. Equation 5 has been derived from dimensional analysis, and is strictly valid for cavity Froude numbers greater than 1 and for small cavitation numbers. Combining Eqs. 4 and 5, one obtains:

$$\frac{\dot{V}}{U_\infty d^2} = C_2 C_{D0} \frac{(1+\sigma)}{\sigma}\sqrt{\frac{1}{\sigma}\ln\frac{1}{\sigma}} \tag{6}$$

The drag coefficient at zero cavitation number, $C_{D0}$, and that corresponding to a nonzero $\sigma$, $C_D$, are related by the following equation[17]:

$$C_D = C_{D0}(1+\sigma) \tag{7}$$

that corresponds to the asymptotic expansion of the drag coefficient formula for small $\sigma$ values.

Finally, introducing Eqs. 7, 3, and 2 in Eq. 6, it follows that:

$$\frac{\dot{V}}{U_\infty d^2} = C_1 C_2 \sqrt{C_{D0}} \frac{\left(1 + C_1\frac{d}{L}\right)^{0.5}}{\left(C_1\frac{d}{L}\right)^{1.5}} \tag{8}$$

Equation 8 provides the relationship of the volumetric flow-rate of the gas phase leaving the cavities, $\dot{V}$, with the

impeller speed, $U_\infty$, the geometrical characteristic length of the cavitator, $d$, the drag coefficient at zero cavitation number, $C_{D0}$, and the length of the cavities, $L$. Therefore, the cavity length can be computed through the above correlation, provided that the flow rate of the gas leaving the cavity is known. It is worth observing that the impeller geometry influences the cavity length through the dimension $d$ and the drag coefficient $C_{D0}$, whereas the sparger geometry plays a role in the cavity length through the gas flow rate, $\dot{V}$.

In this work, the characteristic dimension of the blade, $d$, has been simply assumed to be equal to the blade width, $W$ (i.e., $D/4$ for a standard Rushton turbine), whereas drag coefficient evaluation requires a deeper analysis. For base-cavitation flows, that is, for a cavity attached to the base of the cavitator, as is the case of the impeller blade cavity, the drag coefficient is proportional to the square of the cavitator size.[30] Also, taking into account the drag coefficient dependency on the characteristics of the impeller (i.e., power number, Po, and flow number, Fl), the following equation can be adopted:

$$C_{D0} \propto W^2 \frac{\mathrm{Po}}{\mathrm{Fl}} \tag{9}$$

Therefore, the final form for Eq. 8 is:

$$\frac{\dot{V}}{V_{\mathrm{tip}} W^2} = \overline{C}_2 W \sqrt{\frac{\mathrm{Po}}{\mathrm{Fl}}} \frac{\left(1 + C_1 \frac{W}{L}\right)^{0.5}}{\left(C_1 \frac{W}{L}\right)^{1.5}} \tag{10}$$

The application of Eq. 10 to cavity length estimation is feasible in practice, since all the variables are typically known, apart from the gas flow-rate leaving the cavities, $\dot{V}$, for which suitable correlations and/or simplified assumptions are required, depending on the specific stirred vessel geometrical configuration.

In this work, in order to calculate $\dot{V}$ the whole gas phase flow-rate entering the impeller has been assumed to go out passing through the cavity, without neglecting the influence of gas sparger on the gas phase hydrodynamics. For $D_s$ smaller than $D$, almost all the gas flow rate coming from the sparger enters the turbine, whereas in the opposite case ($D_s > D$) most of the gas fed is distributed into the stirred tank without passing through the impeller. Therefore, in the SS case $\dot{V}$ is equal to the freshly sparged, $Q_g$, plus some recirculated gas, $Q_r$, whereas in the LS case only the recirculated gas flows into the impeller and $\dot{V}$ coincides with $Q_r$.

In any case, the recirculated gas flow rate, $Q_r$, has to be known. For its estimation, the simplified model suggested by Paglianti et al.[15] can be adopted:

$$Q_r = \mathrm{Fl}\ \varepsilon\ \mathrm{ND}^3 - V_b \frac{D^2}{4} \pi \varepsilon (1 - \varepsilon) \tag{11}$$

where $\varepsilon$ is the mean void fraction in the stirred tank and $V_b$ is the bubble rising velocity in a quiescent liquid. Among the possible correlations for the estimation of the mean void fraction, $\varepsilon$, the following equation,[31] that is strictly valid only for a Rushton turbine, was selected:

$$\varepsilon = \frac{V_m^* - V_0}{V_m^* + V_1} \tag{12}$$

where the velocities $V_m^*$, $V_0$ and $V_1$ depend on the geometrical characteristics of the system, the working conditions, and the physical properties of the liquid.[31]

It is worth observing that any specific correlation, that is believed to be reliable for each particular impeller, can be selected for the estimation of $\varepsilon$ as an alternative to Eq. 12. For example, for the case of flat blades, different correlations based on the dependence of $\varepsilon$ on the aerated energy dissipation rate[27,32,33] could be adopted, but iterative calculations would be required.

The area of the single cavity has been always evaluated as $W \times L$, whereas the total volume of the cavities has been computed as the product $N_c \times L \times h \times W$, where $h$ is the blade height and $N_c$ is the number of large cavities formed at the specific experimental conditions. For Rushton turbines, this last has been estimated using the guidelines of Bruijn et al.[1] The same guidelines have also been adopted for curved blades, for which cavity maps are not currently available. Nevertheless, simple experiments for each specific impeller are suggested for precise determination of $N_c$ and consequently of the total volume of the cavities.

In the case of convex blade impellers, the overall cavity volume was considered to be equal to the cavity volume predicted by the model plus the volume contained inside the blade, while for concave blade impellers, if the cavities were present their volume could be evaluated by subtracting the volume included inside the blades from the predicted one.

### *Prediction of power consumption in gas–liquid stirred vessels*

Among the possible applications of the correlation for cavity size, the prediction of power consumption in gas–liquid stirred vessels can be considered, since the drop in power due to the presence of ventilated cavities is a complex problem that has not been extensively modeled yet.[34] As shown by Paglianti et al.,[15] the ratio between $P_g$ and $P_l$, at the same impeller speed, $N$, depends on the density of the two-phase flow inside the impeller blades and can be computed as:

$$\frac{P_g}{P_l} = (1 - \varepsilon_m)(1 - \beta_t) + \frac{\rho_g}{\rho_l}[\varepsilon_m + \beta_t(1 - \varepsilon_m)] \tag{13}$$

where $\rho_g$ and $\rho_l$ are the gas and the liquid density, respectively, $\beta_t$ is the cavity gas hold-up at the impeller disc plane, and $\varepsilon_m$ is the mean void fraction at the turbine, that can be evaluated as:

$$\varepsilon_m = \frac{Q_g + Q_r}{\mathrm{Fl} \cdot N \cdot D^3} \tag{14}$$

The cavity gas hold-up, $\beta_t$, is a function of the number of large cavities, $N_c$, and of the cavity size $W \times L$. Equation 10 can be used for estimating this last parameter and the total gas hold-up of the cavities can be calculated as:

$$\beta_t = \frac{N_c \cdot W \cdot L}{\frac{\pi}{4} D^2 - \frac{\pi}{4}(D - 2W)^2} \tag{15}$$

Equation 15 can be adopted for the loading conditions, while at flooding the cavity gas-hold-up assumes the constant value of 0.5.[15] It is to be noted that for concave blades

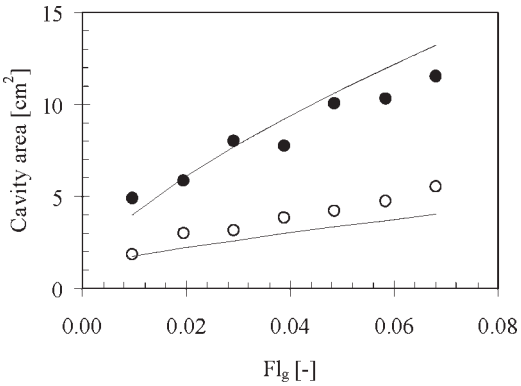


**Figure 5. Comparison between experimental and computed data; effect of the sparger size and of the gas flow number.**

$N$ = 300 rpm. Solid symbols: SS; open symbols: LS; lines: model results (Eq. 10).

impellers, $\beta_t$, is always nil, as a consequence of the absence of large cavities ($N_c = 0$): therefore, at the flooding point a value of mean void fraction $\varepsilon_m$ equal to 0.5 has to be adopted in the model (Eq. 13).

### *Validation of the model*

*Cavity Size.* In Figure 5, a comparison between the measured cavity area and the data computed with Eq. 10 is shown, for a fixed value of the impeller speed and various gas flow-rates. The predictions have been obtained tuning the model constants $C_1$ and $\overline{C}_2$ with the experimental results and their value was fixed at $8.30 \times 10^{-3}$ and $6.04 \times 10^{-3}$ m$^{-1}$, respectively. As can be observed, for both spargers, the suggested model properly allows the evaluation of cavity area. Figure 6 shows a parity plot containing all the experimental data obtained in the present work compared with that predicted by Eq. 10. Even if the model is a simplified representation of the hydrodynamics at the blades, the results are fairly satisfactory.

To provide a further test for the correlation, the experimental data on cavity size collected in the past by Greaves et al.[35] and Warmoeskerken[36] have been considered. In Figure 7, the experimental data of Greaves et al.[35] and the model predictions are compared. A satisfactory agreement can be observed for the $D/T$ = 1/4, while for the other two impeller diameters the model underestimates slightly the measured volume of the cavities; overall, the model predicts the experimental values fairly well.

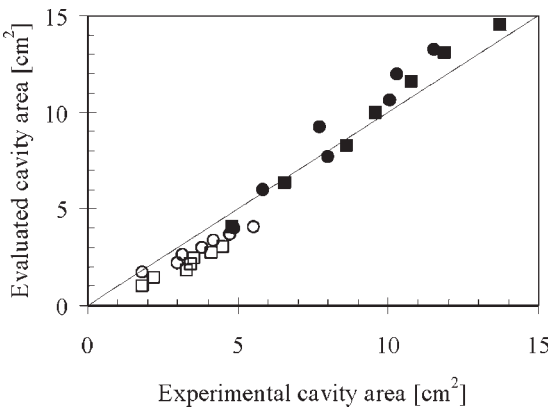


**Figure 6. Comparison between computed and experimental data.**

Symbols as in Figure 2.

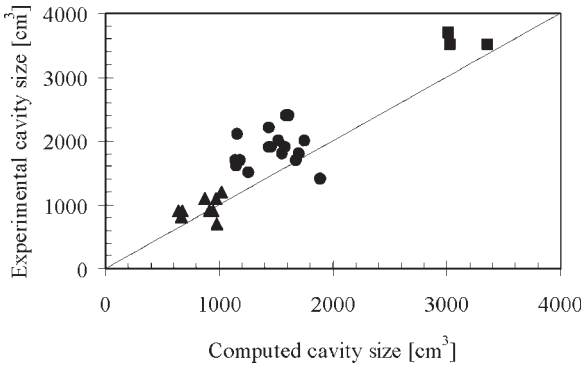


**Figure 7. Comparison between the experimental data by Greaves et al.[35] and the model results (Eq. 10).**

▲, $D/T$ = 1/4; ●, $D/T$ = 1/3; ■, $D/T$ = 1/2.

In Figure 8, the computed and the experimental data of Warmoeskerken[36] are compared. The accuracy of the model is fairly satisfactory also in this case and the model underestimates the cavity size only slightly, the mean square error being less than 14%.

Overall, the model for cavity length estimation provides acceptable predictions in a reasonably wide range of experimental conditions mainly falling in turbulent conditions and in the loading regime. Indirect test of its reliability is provided also from the power consumption previsions reported in the following section.

*Power Consumption in Nonboiling Gas–Liquid Systems.* A comparison between the present experimental power ratios and those computed using Eq. 13, combined with Eqs. 10, 14, and 15, is shown in Figure 9. As can be observed, the proposed model predicts the experimental data with acceptable accuracy independently of the sparger size,

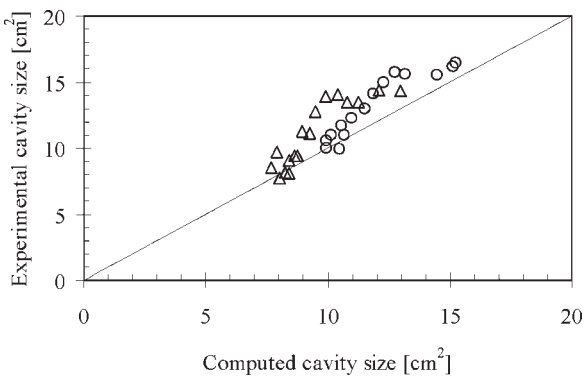


**Figure 8. Comparison between the experimental data by Warmoeskerken[36] and the model results (Eq. 10).**

△, $N$ = 240 rpm; ○, $N$ = 300 rpm.

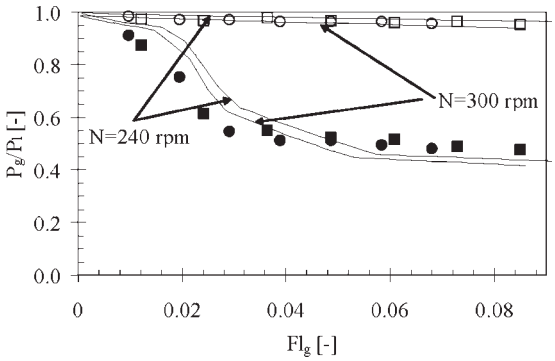


**Figure 9. Comparison between experimental and computed data of $P_g/P_l$.**

Effect of the sparger size and of the gas flow number. ■, SS N = 240 rpm; □, LS N = 240 rpm; ●, SS N = 300 rpm; ○, LS N = 300 rpm; lines: present model.

thus confirming that it properly takes into account the reduction in power consumption due to cavity formation.

It is worth observing that the model for the cavity size (Eq. 10) has been tuned with the experimental data collected in a tank of standard geometry stirred with a Rushton turbine (constants $C_1$ and $\overline{C}_2$). Therefore, its applicability to a wider range of impeller types is not obvious. In the following, this possibility is evaluated with special attention to novel turbines that are increasingly adopted in gas–liquid industrial applications. To assess the model reliability for these additional cases, the experimental data of Vasconcelos et al.[32] have been selected, that provide gassed power consumption for different types of blades (namely flat, convex, concave, and angled blades); the data relevant to the fully turbulent regime are analyzed. For each impeller type, the ungassed impeller flow number, Fl, to be provided in the model (Eq. 10) was assumed to be directly proportional to the ungassed interstage number, given by those authors; for a Rushton turbine Fl is equal to 0.75.

The predicted $P_g/P_l$ values relevant to the Rushton turbine show fair agreement with the experimental power ratio, similar to that of Figure 9, and are therefore omitted for brevity.

Figure 10 shows the comparison between the experimental and computed data for a convex blade impeller, and also for this impeller shape the accuracy of the model seems to be acceptable. The sharp steps in the computed line correspond to the discontinuous change of the total cavity gas hold-up, $\beta_t$, depending on the number of large cavities (see Eq. 15). To this purpose, it can be useful to remind that for Rushton turbines a few investigators[1,37] have reported experimental power ratio discontinuous decrease, corresponding to changes in the number of large cavities. It is worth specifying that the gas hold-up and the number of large cavities have been estimated on the basis of the results obtained for Rushton turbines, since specific information on convex impellers are not available. For future developments, an experimental database for different impellers containing the parameters that are now evaluated with correlations developed for Rushton turbines could be beneficial. Probably, the accuracy of the model could be further improved adopting more precise values relevant to each impeller, but, on the other hand, the lack of such information does not preclude the adoption of the correlation with acceptable confidence.

In the case of concave blade impellers, named Concave, Lancet I, and Lancet II, the presence of cavities should be excluded. To provide a further test to the importance of cavity formation on gassed power, two different hypotheses have been tested: first, power consumption has been calculated assuming no cavity, then cavity existence has been considered. The experimental and computed data for the three different kinds of concave impellers are shown in Figure 11. Though the overall agreement is poorer than in the other cases, it is apparent that allowing the cavity presence makes the model prediction farer from the experiments, thus confirming that a general knowledge of the impeller blade behavior with respect to cavity formation is required. If the cavities are assumed to be absent, the model prediction is closer to the experimental value, though a systematic underestimation of the gassed power consumption is observed, in particular when the experimental $P_g/P_l$ ratio is higher than 1. The experimental increase of gassed power consumption with respect to the single phase system has been explained as a result of bubble presence in the vortex region behind the blades, which increases the drag,[11] or because the introduction of gas does not lead to the formation of gas-filled cavities, but rather disrupts the smooth flow streamlining around the blade.[38] In any case, these local fluid-dynamic effects cannot be forecasted by the simple model suggested in the present work, although the accuracy of the prediction could be improved by empirical methods.[38]

The experimental and computed $P_g/P_l$ ratio for hollow and edge blades obtained by bending plain surfaces by 90° is shown in Figure 12. In both cases, the model predicts the experimental values with sufficient accuracy, confirming that for blades bended by 90° large cavities are present and the model is able to catch their effect on power consumption reduction fairly well.

For impellers with blades bended by an angle equal to 60°, as is the case of concave blades, the experimental data show that up to about $Fl_g = 0.019$ the gassed power consumption is higher than that of the ungassed conditions, as can be observed in Figure 13. Again, the model cannot predict the experimental increment of power consumption. Over-

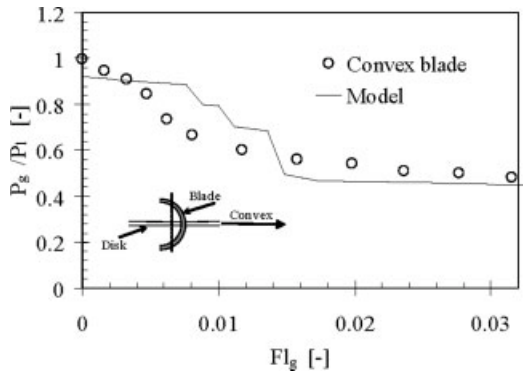


**Figure 10. Comparison between experimental and computed data of $P_g/P_l$.**

Experimental data by Vasconcelos et al.[32] Impeller with convex blades.

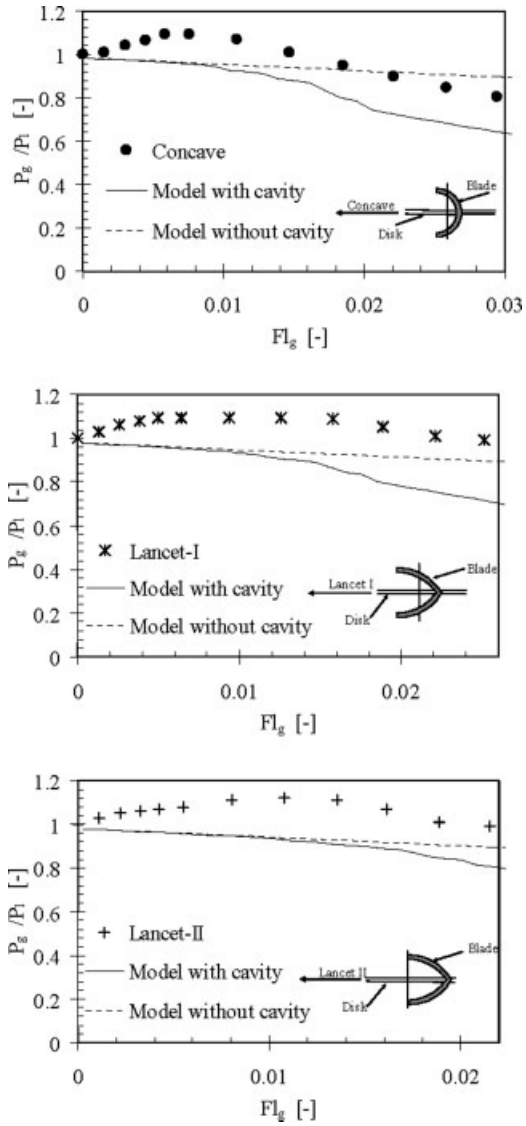


**Figure 11. Comparison between experimental and computed data of $P_g/P_l$.**

Experimental data by Vasconcelos et al.[32] Impellers with concave blades.

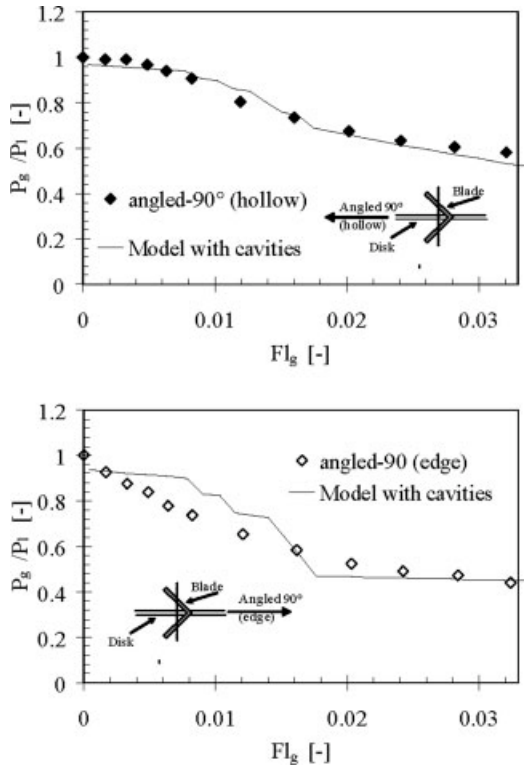


**Figure 12. Comparison between experimental and computed data of $P_g/P_l$.**

Experimental data by Vasconcelos et al.[32] Impellers with hollow and edge blades.

all, the trend computed by neglecting the presence of the cavities provides a better prediction of the experimental behavior thus suggesting that, when the blade angle is low, cavities do not form at the rear of the blades.

Finally, some experimental data obtained by Myers et al.[39] with the CD-6 impeller, a type frequently used in industry, have been analyzed. The accuracy of the model is acceptable (see Figure 14) even if the flooding condition is underpredicted.

In conclusion, the proposed model allows to predict with acceptable accuracy the power consumption in gas–liquid systems stirred by Rushton turbines or by impellers with concave and convex blades. For convex or edge blades, the prediction is slightly worse but still acceptable, at least to a first approximation, provided that cavity absence is assumed as a starting information.

It is finally worth pointing out that the model for cavity length estimation has been tested directly or indirectly, through power consumption data, in all the regions of the Smith's flow map,[40] apart from the regimes of unsatisfactory gas dispersion and flooding, which are of no practical interest. Because of the acceptable accuracy of the predictions obtained in all the cases, we can conclude that our approach can be confidently applied to different regimes.

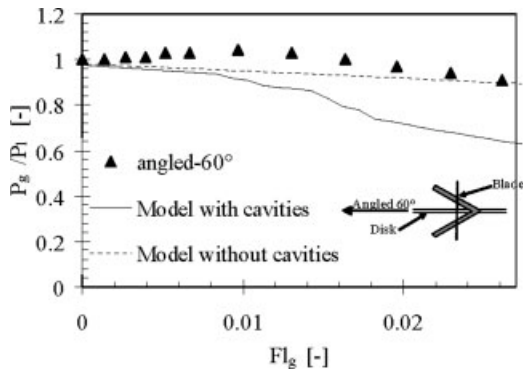


**Figure 13. Comparison between experimental and computed data of $P_g/P_l$.**

Experimental data by Vasconcelos et al.[32] Impeller with blades angled 60°.

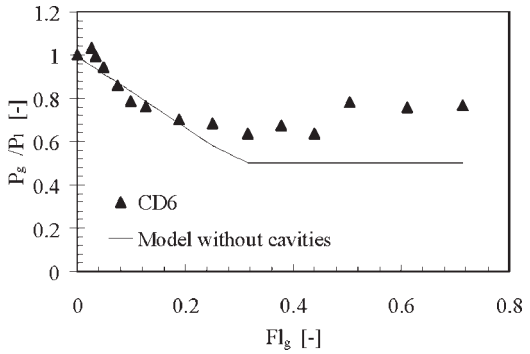


**Figure 14. Comparison between experimental and computed data of $P_g/P_l$.**

Experimental data by Myers et al.[39] CD-6 Impeller.

*Power Consumption in a Boiling Liquid.* Several authors have stressed the similarities between the ventilated cavities formed at the mechanical devices used for gas dispersions and the cavities developed in agitated, unsparged boiling liquids.[20] One of the major differences between the two systems is related to power demand, which is independent of the boiling-up rate[20] in boiling stirred tanks, while it is strictly dependent on the gas flow rate in mechanical gas dispersion. The applicability of the model for the power consumption prevision in boiling systems is worth being examined. To this purpose, one of the variables that should be analyzed is the recirculated vapor that is related to the void fraction. Smith et al.[33] showed that the overall void fraction for boiling liquid is significantly lower than the void fraction characterizing gas–liquid systems, and consequently, in boiling liquids the vapor does not load the impeller as a noncondensable gas does.[20] As a result, it seems reasonable to neglect vapor recirculation in the model for the power consumption, while still considering the cavity effect.

It is also important to recall that the model for cavity size estimation (Eq. 10) was based on correlations with the cavitation number $\sigma$, while for stirred boiling systems the Smith number, Sm, is often adopted.[41,42] This last is defined as the ratio between 2Sg and $V_{tip}^2$, where S is the impeller submergence below free surface and $g$ is the acceleration of gravity. For a boiling liquid, the cavitation number definition nearly matches that of the Smith number, although some differences between the two dimensionless numbers arise because the pressure within the vapor cavity is affected by both local fluid mechanics and thermal factors.[42] Since the typical range of Smith number in boiling systems is 0.2–4, Eq. 2, and the simplified form given by Eq. 3, cannot be used. Therefore, an attempt to adopt the correlation provided by Lindau et al.[43] can be performed, according to whom for $\sigma$ between 0.01 and 1, the cavity size can be evaluated as:

$$\frac{L}{WC_D} = C_3\sigma^{C_4} \tag{16}$$

Using Eq. 7 and considering that in a boiling system $\sigma$ fairly matches the Smith number, the previous equation can be rewritten as:

$$\frac{L}{W} = C_3\mathrm{Sm}^{C_4}C_{D0}(1+\mathrm{Sm}) \tag{17}$$

and finally introducing Eq. 9, the final form of Eq. 17 is:

$$\frac{L}{W} = \overline{C}_3\mathrm{Sm}^{C_4}W^2\frac{\mathrm{Po}}{\mathrm{Fl}}(1+\mathrm{Sm}) \tag{18}$$

The constants $\overline{C}_3$ and $C_4$ have been tuned with the experimental data collected by Smith and Katsanevakis[42] for a Rushton turbine and take the values of 13.8 $m^{-2}$ and $-2.09$, respectively.

Focusing on radial impellers, Smith et al.[41] published experimental power consumption data for the Rushton, the CD-6 and the BT-6 turbines. As pertains the CD-6 and the BT-6 impellers, no cavities form at the rear of the blades, due to their concave shape. For the Rushton turbine, the six-symmetric configuration has been assumed, in which all six cavities are large and of similar size[44]; when the turbine is flooded, the cavity gas-hold-up was assumed to be equal to the constant value 0.5.

For the convex blade impeller, the same hypothesis introduced for gas–liquid systems has been used: the cavity size was evaluated by adding the volume included inside the blades to that obtained by the model equation.

The model adequacy in predicting the power consumption in boiling systems can be evaluated from Figure 15, where the predicted curves are compared with the experimental data of Smith and Katsanevakis[42] and Smith et al.[41] In all cases, the accuracy of the model seems to be acceptable. For the case of concave blade impellers, for which the present model calls for cavity absence, the experimental $P_g/P_1$ ratio remains approximately equal to one, whereas for the Rushton turbine and for the convex blade turbines, for which the cavities are present, the experimental $P_g/P_1$ values sharply decrease when decreasing the Smith number.

The experimental data shown in Figure 15 confirm our criterion of excluding the cavity presence with concave blades. This result disagrees with the experimental data of Smith and Katsanevakis,[42] who obtained experimental $P_g/P_1$ data lower than 0.6 for a concave blade impeller. As pointed out by Smith et al.,[41] this discrepancy could be due to the particular subtended angle of the blades used.

Finally, it is worth noting that, with the present model, the presence of salt in the liquid phase does not influence the

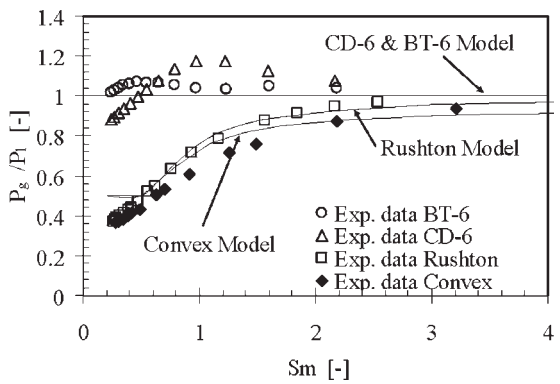


**Figure 15. Comparison between experimental and computed data of $P_g/P_l$.**

Experimental data by Smith and Katsanevakis[42] and Smith et al.[41] Boiling systems; BT-6, CD-6, Rushton and convex impellers.

value of the cavity size, because it does not change the cavitation number. This result agrees with the experimental data of Smith and Tarry,[45] who showed that for a Rushton turbine the relative power demand in a boiling salt solution is the same as that obtained with clean water.

In conclusion, the proposed model, based on the evaluation of the size of the large cavities, allows to predict the power consumption in gas–liquid and in boiling systems with sufficient accuracy. For predicting the power consumption, two fitting parameters have been used for the gas–liquid systems and another two for the boiling systems, but these parameters do not depend on the impellers characteristics or on tank geometry.

## Conclusions

A mechanistic model has been suggested to evaluate the ventilated cavity size forming behind the impeller blades in gas–liquid systems. The experimental data show that the dimensions of the cavities are strongly dependent on the sparger size. If the sparger diameter is smaller than that of the impeller, the whole fresh gas stream coming from the sparger goes to the impeller and induces the formation of large ventilated cavities. While, if the sparger diameter is much larger than that of the impeller, the gas flowing into the impeller is mainly due to recirculation and, in this case, the cavity size is smaller. The cavity presence strongly affects power consumption: the power drawn under aeration obtained with LS is much lower than that induced by SS at equal sparged flow rate, while the effect on the whole mean void fraction in the vessel seems to be negligible. The cavity size can be easily predicted using an analogy with the theory developed for evaluating the behavior of the ventilated cavities at the rear of vehicles. Once the above model is associated to a mechanistic model describing the hydrodynamics of the two-phase mixtures, the power consumption of the impeller working with gassed or boiling systems can be evaluated without introducing any adjustable parameters. The model developed for a Rushton turbine has been extended to radial impellers of more industrial significance. Finally, improvements to the prediction accuracy could be expected as soon as a more detailed knowledge on the cavity structure for any specific impeller will be available.


## Acknowledgments

This work was financially supported by the Italian Ministry of University and Research (MIUR) and the University of Bologna under PRIN program. The valuable advice of Prof. Franco Magelli is gratefully acknowledged.


## Notation

$B$ = baffle width, m
$C$ = impeller off-bottom clearance, m
$C_D$ = drag coefficient, dimensionless
$C_{D0}$ = drag coefficient at zero cavitation number, dimensionless
$C_s$ = sparger off-bottom clearance, m
$C_1$ = constant in Eq. 3, dimensionless
$C_2$ = constant in Eq. 5, dimensionless
$\bar{C}_2$ = constant in Eq. 10, $m^{-1}$
$C_3$, $C_4$ = constant in Eq. 16, dimensionless
$\bar{C}_3$ = constant in Eq. 18, $m^{-2}$
$d$ = cavitator length, m
$D$ = impeller diameter, m
$D_s$ = sparger diameter, m
Fl = impeller flow number, dimensionless
$Fl_g$ = gas flow number, dimensionless
$g$ = acceleration of gravity, m $s^{-2}$
$h$ = blade height
$H$ = liquid height, m
$L$ = cavity length, m
$N$ = impeller rotational speed, $s^{-1}$
$N_c$ = number of large cavities, dimensionless
$p_\infty$ = free stream pressure, Pa
$p_c$ = cavity pressure, Pa
$P_g$ = gassed power consumption, W
$P_l$ = ungassed power consumption, W
Po = impeller power number, dimensionless
$\bar{Q}$ = gas entrainment coefficient, dimensionless
$Q_g$ = gas flow rate, $m^3$ $s^{-1}$
$Q_r$ = recirculated gas flow rate, $m^3$ $s^{-1}$
Sm = Smith number, dimensionless
$T$ = tank inner diameter, m
$U_\infty$ = undisturbed free stream velocity, m $s^{-1}$
$\dot{V}$ = volumetric gas flow leaving the cavity, $m^3$ $s^{-1}$
$V_b$ = bubble rising velocity in quiescent liquid, m $s^{-1}$
$V_m^*$ $V_0$ $V_1$ = velocities in Eq. 12, m $s^{-1}$
$V_{tip}$ = impeller blade tip velocity ($=\pi ND$), m $s^{-1}$
$W$ = impeller blade width, m

### *Greek letters*

$\beta_t$ = cavity gas hold-up, dimensionless
$\varepsilon$ = mean void fraction, dimensionless
$\varepsilon_m$ = mean void fraction at the turbine, dimensionless
$\rho$ = density, kg $m^{-3}$
$\sigma$ = cavitation number, dimensionless

### *Subscripts*

$g$ = gas
$l$ = liquid

## Literature Cited


1. Bruijn W, van't Riet K, Smith JM. Power consumption with aerated rushton turbines. *Trans Inst Chem Eng*. 1974;52:88–104.
2. Manning SA, Jameson GJ. A study of ventilated gas cavities on disc-turbine blades. *Proceedings of the 7th European Conference on Mixing*, Brugge, BHRA Fluid Engineering Cranfield (U.K.) 1991:225–231.
3. Nienow AW, Wisdom DJ, Middleton JC. The effect of scale and geometry on flooding, recirculation, and power in gassed stirred tank. *Proceedings of the 2nd European Conference on Mixing*, Cambridge, BHRA Fluid Engineering Cranfield (U.K.) 1977; paper F1.
4. Sensel ME, Myers KJ, Fasano JB. Gas dispersion at high aeration rates in low to moderately viscous newtonian liquids. *AIChE Symp Ser*. 1993;89:76–84.
5. Smith JM, Warmoeskerken MMCG. The dispersion of gases in liquids with turbines. *Proceedings of the 5th European Conference on Mixing*, Würzburg, BHRA, 1985:115–126.
6. Warmoeskerken MMCG, Smith JM. Flooding of disk turbines in gas-liquid dispersion—a new description of the phenomenon. *Chem Eng Sci*. 1985;40:2063–2071.
7. Warmoeskerken MMCG, Speur J, Smith JM. Gas-liquid dispersion with Pitched blade turbines. *Chem Eng Commun*. 1984;25:11–29.
8. Bakker A, Van den Akker HEA. Gas-liquid contacting with axial flow impellers. *Chem Eng Res Des*. 1994;72:573–582.
9. Sardeing R, Aubin J, Poux M, Xuereb C. Gas-liquid mass transfer influence of sparger location. *Chem Eng Res Des*. 2004;82:1161–1168.
10. Rewatkar VB, Joshi JB. Role of sparger design on gas dispersion in mechanically agitated gas-liquid contactors. *Can J Chem Eng*. 1993; 71:278–291.

11. McFarlane CM, Zhao X-M, Nienow AW. Studies of high solidity ratio hydrofoil impellers for aerated bioreactors. II. Air-water studies. *Biotechnol Prog*. 1995;11:608–618.
12. Scargiali F, D'Orazio A, Grisafi F, Brucato A. Modelling and simulation of gas-liquid hydrodynamics in mechanically stirred tanks. *Chem Eng Res Des*. 2007;85:637–646.
13. Khopkar AR, Ranade VV. CFD simulation of gas-liquid stirred vessel: VC, S33, and L33 flow regimes. *AIChE J*. 2006;52:1654–1672.
14. Montante G, Paglianti A, Magelli F. Experimental analysis and computational modelling of gas-liquid stirred vessels. *Chem Eng Res Des*. 2007;85:647–653.
15. Paglianti A, Takenaka K, Bujalski W. Simple model for power consumption in aerated vessels stirred by Rushton disc turbines. *AIChE J*. 2001;47:2673–2683.
16. Rigby GD, Evans GM, Jameson GJ. Cavity formation behind ventilated impeller blades. *Recents Progres en genie des procedes*. 1997;11:231–238.
17. Garabedian PR. Calculation of axially symmetric cavities and jets. *Pacific J Math*. 1956;6:611–684.
18. Spurk JH. On the gas loss from ventilated supercavities. *Acta mechanica*. 2002;155:125–135.
19. Spurk JH. Effect of gas temperature on the gas loss from ventilated cavities. *Acta mechanica*. 2004;172:75–81.
20. Middleton JC, Smith JM. Gas-liquid mixing in turbulent systems. In: Paul EL, Atiemo-Obeng VA, Kresta SM, editors. *Handbook of Industrial Mixing Science and Practice*. Hoboken, NJ: Wiley, 2004: 612–617.
21. Nienow AW, Warmoeskerken MMCG, Smith JM, Konno M. On the flooding/loading transition and the complete dispersal condition in aerated vessel agitated by a Rushton turbine. *Proceedings of the 5th European Conference on Mixing*, Wurzburg, BHRA Fluid Engineering (Cranfield (U.K.) 1985:143–154.
22. Machon V, Vlcek J, Skrivanek J. Dual impeller systems for aeration of liquids: an experimental study. *Proceedings of the 5th European Conference on Mixing*, Wurzburg, BHRA Fluid Engineering (Cranfield (U.K.) 1985:155–170.
23. Birch D, Ahmed N. The influence of sparger design and location on gas dispersion in stirred vessels. *Chem Eng Res Des*. 1997;75:487–496.
24. Jia L, Wang C, Wei Y, Wang H, Zhang J, Yu K. Numerical simulation of artificial ventilated cavity. *J Hydrodyn*. 2006;18:273–279.
25. Thiagarajan K, Shock R. Investigation into a ventilated hydrofoils for ride control of high-speed craft. *Proceedings. of the 22nd Symposium on Naval Hydrodynamics*, Washington, DC, National Academic Press, 1999;100–108.
26. Brenner CE. *Cavitation and Bubble Dynamics*. New York: Oxford University Press, 1995.
27. Saito F, Nienow AW, Chatwin S, Moore IPT. Power, gas dispersion and homogenisation characteristics of scaba SRGT and Rushton turbine impellers. *J Chem Eng Jpn*. 1992;25:281–287.
28. Marshall EM, Bakker A. Computational fluid mixing. In: Paul EL, Atiemo-Obeng VA, Kresta SM, editors. *Handbook of Industrial Mixing Science and Practice*. Hoboken, NJ: Wiley, 2004:330–332.
29. Kshatriya SS, Patwardhan AW, Eaglesham A. Experimental studies of ventilated cavities in a channel. *Chem Eng Sci*. 2007;62:979–989.
30. Varghese AN, Uhlman JS, Kirschner IN. Numerical analysis of high-speed bodies in partially cavitating axisymmetric flow. *J Fluids Eng*. 2005;127:41–54.
31. Paglianti A, Takenaka K, Bujalski W, Takahashi K. Estimation of gas hold-up in aerated vessels. *Can J Chem Eng*. 2000;78:386–392.
32. Vasconcelos JMT, Orvalho SCP, Rodrigues AMA, Alves SS. Effect of blade shape on the performance of six-bladed disk turbine impellers. *Ind Eng Chem Res*. 2000;39:203–213.
33. Smith JM, Gao Z, Muller-Steinhagen H. The effect of temperature on the void fraction in the gas-liquid reactors. *Exp Therm Fluid Sci*. 2004;28:473–478.
34. Nienow AW. Gas-liquid mixing studies: a comparison of Rushton turbines with some modern impellers. *Chem Eng Res Des*. 1996;74: 417–423.
35. Greaves M, Barigou M, Brucato A. Power dynamics and cavity formation. *Proceedings of the International Colloquium on Mechanical Agitation*, Toulouse, ENSIGC 1986:4.28–4.35.
36. Warmoeskerken MMCG. Gas-liquid dispersing characteristics of turbine agitators. PhD Thesis, University of Delft, The Netherlands, 1986.
37. Ismail AF, Nagase Y, Imon J. Power characteristics and cavity formation in aerated agitations. *AIChE J*. 1984;30:487–489.
38. Nienow AW, Bujalski W. Recent studies on agitated three phase (gas-solid-liquid) systems in the turbulent regime. *Chem Eng Res Des*. 2002;80:832–838.
39. Myers KJ, Janz EE, Fasano JB. Gas dispersion capabilities on the CD-6 Impeller. *Proceedings of the 12th European Conference on Mixing*, Bologna, AIDIC, 2006:169–176.
40. Smith JM, Warmoeskerken MMCG, Zeef E. Flow conditions in vessels dispersing gases in liquid with multiple impellers. In: Ho CS, Oldshue JY, editors. *Biotechnology Processes: Scale-up and mixing*. New York: AIChE, 1987:107–115.
41. Smith JM, Gao Z, Middleton JC. The unsparged power demand of modern gas dispersing impeller in boiling liquids. *Chem Eng J*. 2001;84:15–21.
42. Smith JM, Katsanevakis AN. Impeller power demand in mechanically agitated boiling. *Chem Eng Res Des*. 1993;71:145–152.
43. Lindau JW, Kunz RF, Boger DA. Stinebring DR, Gibeling HJ. Validation of High Reynolds Number, Unsteady multi-phase CFD modeling for naval applications. *Proceedings of the 23rd Symposium on Naval Hydrodynamics*, Val de Reuil, France, 2000:423–435.
44. Smith JM, Verbeek DGF. Impeller cavity development in near boiling liquids. *Chem Eng Res Des*. 1988;66:39–46.
45. Smith JM, Tarry K. Impeller power demand in boiling solutions. *Chem Eng Res Des*. 1994;72:739–740.

*Manuscript received Feb. 22, 2007, revision received Sept. 24, 2007, and final revision received Nov. 29, 2007.*